

GA-A23721

**ADVANCED TOKAMAK MODELING BASED ON
DIII-D ECCD EXPERIMENTS AND FLUX
EVOLUTION MEASUREMENTS**

by

**H.E. ST. JOHN, M. MURAKAMI, T.A. CASPER, R.H. COHEN,
J. FREEMAN, R.A. JONG, T.B. KAISER, J.E. KINSEY, L.L. LAO,
Y.R. LIN-LIU, L.L. LoDESTRO, and L.D. PEARLSTEIN**

AUGUST 2001

DISCLAIMER

This report was prepared as an account of work sponsored by an agency of the United States Government. Neither the United States Government nor any agency thereof, nor any of their employees, makes any warranty, express or implied, or assumes any legal liability or responsibility for the accuracy, completeness, or usefulness of any information, apparatus, product, or process disclosed, or represents that its use would not infringe privately owned rights. Reference herein to any specific commercial product, process, or service by trade name, trademark, manufacturer, or otherwise, does not necessarily constitute or imply its endorsement, recommendation, or favoring by the United States Government or any agency thereof. The views and opinions of authors expressed herein do not necessarily state or reflect those of the United States Government or any agency thereof.

ADVANCED TOKAMAK MODELING BASED ON DIII-D ECCD EXPERIMENTS AND FLUX EVOLUTION MEASUREMENTS

by

H.E. ST. JOHN, M. MURAKAMI,[†] T.A. CASPER,[‡] R.H. COHEN,[‡]
J. FREEMAN, R.A. JONG,[‡] T.B. KAISER,[‡] J.E. KINSEY, L.L. LAO,
Y.R. LIN-LIU, L.L. LoDESTRO,[‡] and L.D. PEARLSTEIN[‡]

This is a preprint of a paper to be presented at the 28th
European Physical Society Conference on Plasma
Physics in Controlled Fusion, Madeira, Portugal,
June 18-22, 2001 and to be published in the *Proceedings*.

[†]Oak Ridge National Laboratory

[‡]Lawrence Livermore National Laboratory

Work supported by
the U.S. Department of Energy under
Contracts DE-AC03-99ER54463, W-7405-ENG-48
and DE-AC05-76OR00033

GENERAL ATOMICS PROJECT 30033
AUGUST 2001

ADVANCED TOKAMAK MODELING BASED ON DIII-D ECCD EXPERIMENTS AND FLUX EVOLUTION MEASUREMENTS

H.E. St. John,¹ M. Murakami,² T.A. Casper,³ R.H. Cohen,³ J. Freeman,¹ R.A. Jong,³
T.B. Kaiser,³ J.E. Kinsey,¹ L.L. Lao,¹ Y.R. Lin-Liu,¹ L.L. LoDestro,³
and L.D. Pearlstein,³

¹General Atomics, P.O. Box 85608, San Diego, California 92186-5608 USA

²Oak Ridge National Laboratory, Oak Ridge, Tennessee, USA

³Lawrence Livermore National Laboratory, Livermore California 94551-0808, USA

INTRODUCTION AND SUMMARY

In this paper we present the initial results of the LLNL/GA transport modeling collaboration. The first goal of this project was to produce a common environment in which the GA and LLNL transport analysis suite of codes could be used advantageously in a cooperative manner. We present the modeling methods developed first to benchmark against experimental results and second, to the simulation of high performance AT scenarios using electron cyclotron current drive (ECCD) that should be achievable experimentally in DIII-D. The results are sensitive to the on-axis beam driven current modeling. We have applied loop voltage analysis methods and found that current kinetic MHD fitting will have to be refined in order to reduce the uncertainty in the beam driven current to useful limits. The quiescent double barrier (QDB) H-mode discovered in DIII-D has implications for long term AT discharge modeling. Some of our initial modeling and stability results of a DIII-D QDB discharge are presented. The long term plan of this project is to eventually merge with the National Transport Code Collaboratory (NTCC).

MODELING AND RESULTS

AT modeling requires that we have confidence in the total predicted current density and in the non-inductive driven currents. We have found that the bootstrap and ECCD driven currents are predicted to a satisfactory degree by existing models and codes. Although not shown in this paper explicitly we have compared the leading bootstrap current models [1,2], in our AT scenario modeling and found the effect of different approximations to the collisionality and geometry to be less than about ten percent in the total bootstrap current for this work. However the on-axis beam driven current is subject to significant variability depending on whether or not prompt orbit averages or full Monte-Carlo slowing down calculations with anomalous spatial diffusion is done. We have observed that for DIII-D discharge 99411, the inclusion of anomalous diffusion in TRANSP calculations can decrease the on-axis beam driven current by as much as forty percent with a constant fast ion diffusion coefficient $D_f = 0.3 \text{ m}^2/\text{s}$. In Fig. 1 we show the steady-state time averaged decrease of the on-axis fast ion current density as a function of D_f . The variation in the steady-state case is due to the Monte-Carlo nature of the calculations.

The total stored (kinetic) energy and the neutron rate are the two primary quantities available for the verification of the fast ion distribution in DIII-D. We show the neutron rate in Fig. 2 with the fast ion diffusion value as a parameter. The stored energy density is not shown but produces results consistent with the observations in Fig. 2. Both of these diagnostics are thought to have an inherent uncertainty of 10–15%. We conclude from these results that a value of $D_f \approx 0.3 \text{ m}^2/\text{s}$ is acceptable.

Ideally we would like to be able to determine the non-inductive current profile from experimental measurements. At present the only way to achieve this result is to use the loop voltage analysis method. The method was originally described in [3] and was subsequently made part of the transport analysis scheme where it is known as the TDEM (time dependent eqdsk) mode of operation. The method is based on the fact that the poloidal flux (divided by 2π) can be shown to satisfy the equation:

$$\frac{\partial}{\partial t} \psi(\rho, t) = CR_0 \eta \left\langle \frac{\vec{J}_{\text{ohmic}} \cdot \vec{B}}{B_{T0}} \right\rangle \quad (1)$$

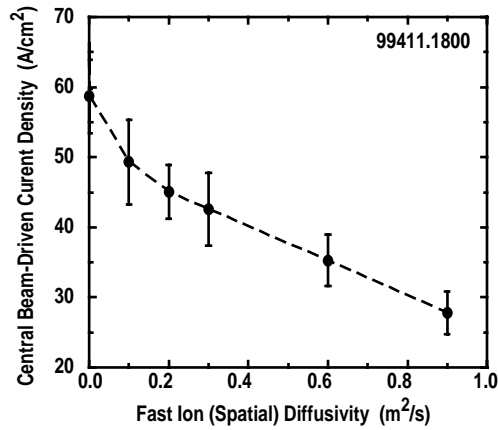


Fig. 1. On-axis neutral beam current drive for shot 99411 at 1800 ms.

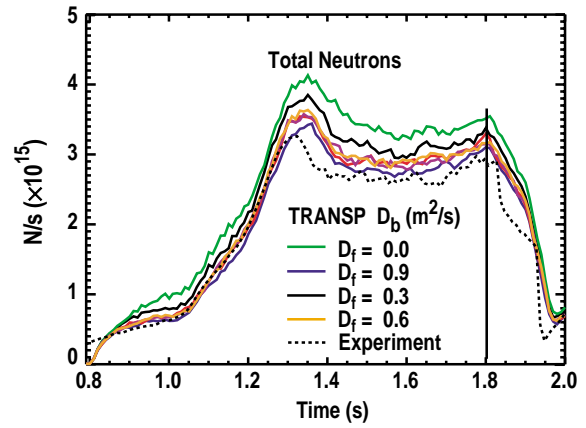


Fig. 2. Experimental and calculated neutron rate as a function of time for shot 99411.

where η is the parallel resistivity and the quantity in brackets is the flux surface average parallel ohmic current density. The factor C is a metric coefficient depending on the flux surface shape. In the TDEM mode we view the lhs of Eq. (1) as an experimentally determined quantity and hence the product of the resistivity and the ohmic current density becomes a known function of the spatial variable, ρ (which we take to be proportional to the square root of the toroidal flux). Thus, if it is assumed that the neoclassical resistivity is known, then a value for the ohmic current density becomes available. Furthermore, for DIII-D the toroidal current density is known from the detailed free boundary equilibrium calculations based on recursively fitting p' and ff' to measured values of the electron densities, electron and ion temperatures, various magnetic probe and ψ loop measurements and radially resolved motional Stark effect (MSE) measurements. This yields a total toroidal current density which is used in our transport codes directly. Thus we know the total and ohmic current density profiles from experiment. The total current density is just the sum of ohmic and non-inductive driven currents (eg. bootstrap, beam, rf). Hence it is possible to solve for the noninductive current by using the experimental values of the total and ohmic currents. To illustrate the method and its current limitations we apply it to DIII-D shot 99411 at 1800 ms. This shot is an NCS discharge but the TDEM method is more generally applicable. As indicated above the determination of the fast ion current density near the magnetic axis is of paramount interest to us. Consequently we have applied the TDEM method to the determination of the on-axis beam driven current. The remaining non-inductive current contribution for this shot is due to the bootstrap current, whose contribution near the magnetic axis is small. Essentially negligible differences in the on-axis beam driven current were observed due to switching between the Houlberg [1] and Sauter [2] bootstrap models (the primary effect here enters through the resistivity, which is slightly different for the two bootstrap models). However a considerable variation in the resulting on-axis beam driven current was obtained when the time interval over which the fit to the time derivative of ψ was performed. Averaging these results together leads to an on-axis beam driven current value of 62.4 ± 36.3 amps cm^2 . Hence the TDEM method is consistent with a fast ion anomalous diffusion coefficient as large as about $1 \text{ m}^2/\text{s}$.

We used the Monte-Carlo Guiding center Orbit (MCGO) code to verify our calculated beam deposition. MCGO solves the steady-state slowing down problem of fast ions colliding with a thermal background of electrons, ions and neutrals. As indicated by the name the actual guiding center orbit of fast ions is determined in (R, ϕ, z) geometry with real wall and limiter placement possible. Typically a total of 5000 ions, appropriately split into full, half and third energy components, are chosen from the initial birth profile of fast ions provided by the Monte-Carlo fast ion deposition code NFREYA. MCGO does not currently have the ability to include additional anomalous spatial diffusion. However we can approximately account for this effect by spreading the NFREYA deposition pattern that MCGO samples. The orbit of the injected ions is periodically interrupted and the amount of energy delivered to the background plasma (or absorbed from the plasma with a small but non vanishing probability) during the last time step is determined. The pitch angle of the ion is then

modified by sampling from a probability distribution that has the same mean and variance as the pitch angle operator used in the Fokker Planck approach. Probabilities against charge exchange and fusion are also determined at this time and the ion orbit is terminated if such an event occurs. If the ion charge exchanges to become a neutral the trajectory of the neutral is followed until it hits the wall or re-ionizes. The fast ion neutron rates calculated by MCGO were combined with the thermonuclear rates determined from the thermal transport code to obtain the total neutron rate. These calculations differed from the zero fast ion diffusion results shown in Fig. 2 by no more than 15%, placing them within the expected experimental error associated with the neutron rate measurements. As is seen in Fig. 2 this does not rule out higher values of the fast ion diffusion coefficient however.

Using the experimentally determined values of the thermal diffusivities for shot 99411 at 1800 ms we show the result of one steady-state AT prediction in Fig. 3. In this simulation we evolved the electron and ion temperatures and the plasma current for a period of 25 s, starting with the experimental initial conditions at 1.8 s. As is observed in Fig. 2 based on the neutron rate and also confirmed by total stored energy values obtained from kinetic MHD fitting, a value of $0.3 \text{ m}^2/\text{s}$ for the fast ion diffusion coefficient best fits the experimental results. Accordingly the MCGO code was given an initial smoothed deposition from NFREYA which approximately corresponded to this value. The power delivered to the electrons and ions and the neutral beam driven current were then determined by MCGO and fed back into the transport code. This results in the final on-axis beam driven current of about 30 A/cm^2 shown in Fig. 3. We note that without this procedure our on-axis neutral beam current would have been significantly larger, approximately 70 A/cm^2 . Both values are within the TDEM approximation given above but the lower value is supported by the stored energy and neutron rate values. The simulation was done with both the Houlberg [1] and Sauter [2] bootstrap current formulations. The Sauter model approximates the collision operator more accurately and hence may be more acceptable near the plasma edge. However, for our current results this turned out not to be an issue since the models differed by less than 5 A/cm^2 near the plasma edge. The choice of EC current drive location just inside the peak of the bootstrap current profile was previously shown to be favorable for optimal stability considerations [4]. The toroidal electric field associated with this result after 25 s of simulation is shown in Fig. 4. The electric field is sufficiently flat at this time that we do not expect much further change in the ohmic current given in Fig. 3. The experimental and final q profiles are also indicated in Fig. 4. The final q profile has a minimum above 2.5 with a small hump near $r = 0.45$. This structure is due to the Gaussian shape of the rf current deposition shown in Fig. 3. We used a single rf gyrotron simulation for this case. Fine tuning of the EC current profile is possible by using more than one gyrotron with slightly different launch geometries. Hence, the structure of the q profile near the minimum q is controllable. Balloning and $n=1$ kink mode stability was verified for this scenario using the BALOO and GATO codes. The AT modeling results are summarized in Table 1.

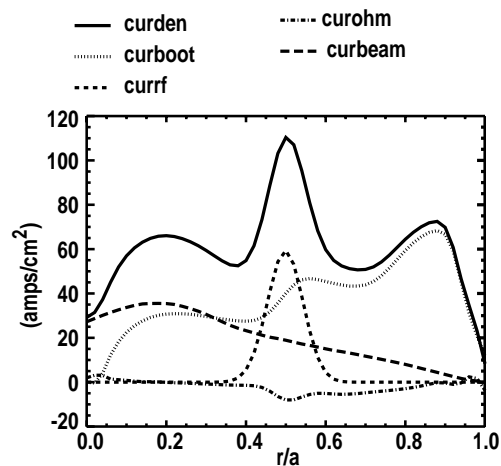


Fig. 3. Near steady-state total (curden), ohmic (curohm), bootstrap (curbeam) and ECCD (curr) current profiles for AT modeling of shot 99411.

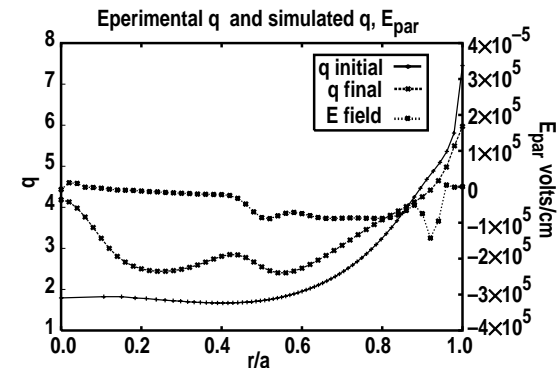


Fig. 4. The q profile at the start and in steady-state and the near equilibrium toroidal electric field for the AT case of Fig. 3.

Table 1
Shot 99411 AT Modeling Results

$\beta_N = 3.95$	Balloning stable (BALOO)
$\beta_{NH} = 11.85$	n=1 kink stable with DIII-D conducting wall at 1.5 a (GATO)
$\beta_p = 1.73$	
$I_p = 1.19$ MA	
$I_{boot} = 0.82$ MA	
$I_{ECCD} = 0.15$ MA	$P_{ECH} = 3.0$ MW
$I_{beam} = 0.28$ MA	$P_{beam} = 6.17$ MW

Further prospects in AT scenario modeling became possible with the discovery of the quiescent, double barrier (QDB) mode of operation [5]. The QDB mode is of current interest due to its near steady discharge conditions for long duration, 3 sec in DIII-D without ECH. The formation of a double barrier, a core transport barrier with an H-mode-like pedestal, results in high performance discharges. Quiescent, ELM-free operation maintains sufficient edge particle transport due to a quasi-coherent edge mode that provides coupling to the divertor pumps required for density control. Electron temperature and density profiles are consistent with conditions where electron cyclotron (EC) power absorption and current drive efficiency are good. Further simulations are exploring scenarios for improving performance and for extensions to steady-state. The TORAY-GA EC ray tracing code is used for EC current drive with DCON for assessing stability. Three EC sources are used to broaden the deposition and current drive profiles using 0.5 MW/source consistent with power and launchers available on DIII-D. We find that the core q -profile can be controlled at fixed q_{95} with q_{min} maintained near 1.5. Stability analysis of the resulting q and pressure profiles (with measured χ_i, χ_e) at 3 s indicates stability to ideal modes provided the DIII-D conducting wall is included but unstable to n=1 without. The EC-modified discharge simulated remains Mercier stable but stable to resistive interchange and ideal ballooning as well, illustrated in Fig. 5. A Δ' calculation in the large aspect ratio approximation indicates the potential for Rutherford island growth. Ongoing additional simulations form the basis for proposed experiments.

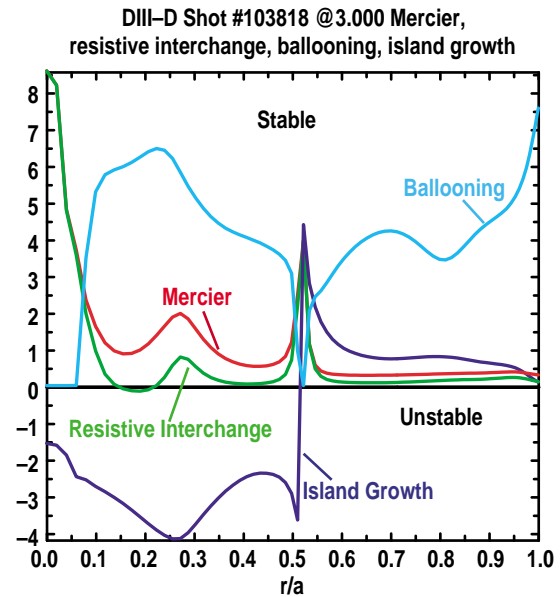


Fig. 5. DIII-D QDB shot 103818 stability growth rates. Negative indicates instability.

ACKNOWLEDGMENT

Work supported by U.S. Department of Energy under Contracts DE-AC03-99ER54463, W-7405-ENG-48, and DE-AC05-00OR22725.

REFERENCES

- [1] W.A. Houlberg, et al. Phys. Plasmas, Vol. 4, No. 9, (1997) 3242.
- [2] O. Sauter, et al., Phys. Plas. Vol. 6, No. 7, (1999) 2384.
- [3] C.B. Forest et al., Phys. Rev. Lett. (1994) 2444.
- [4] M. Murakami, et al., Nucl. Fusion, Vol. 40, No. 6, (2000) 1257.
- [5] C.M. Greenfield et al., Phys. Rev. Lett., Vol. 86, No. 20, (2001) 4544.